



Deposited via The University of Leeds.

White Rose Research Online URL for this paper:

<https://eprints.whiterose.ac.uk/id/eprint/119380/>

Version: Accepted Version

Article:

Rasool, B, McGowan, J, Pastock, D et al. (2017) Redox control of aphid resistance through altered cell wall composition and nutritional quality. *Plant Physiology*, 175 (1). pp. 259-271. ISSN: 0032-0889

<https://doi.org/10.1104/pp.17.00625>

Reuse

Items deposited in White Rose Research Online are protected by copyright, with all rights reserved unless indicated otherwise. They may be downloaded and/or printed for private study, or other acts as permitted by national copyright laws. The publisher or other rights holders may allow further reproduction and re-use of the full text version. This is indicated by the licence information on the White Rose Research Online record for the item.

Takedown

If you consider content in White Rose Research Online to be in breach of UK law, please notify us by emailing eprints@whiterose.ac.uk including the URL of the record and the reason for the withdrawal request.

Short title: Apoplast-associated aphid resistance

Corresponding authors:

Christine H. Foyer

Centre for Plant Sciences, School of Biology, Faculty of Biological Sciences, University of Leeds, LS2 9JT. United Kingdom.

Telephone: +44 113 343 1421

Email: C.Foyer@leeds.ac.uk

Robert D. Hancock

Cell and Molecular Sciences, The James Hutton Institute, Invergowrie, Dundee DD2 5DA. United Kingdom.

Telephone: +44 1382 568 779

Email: rob.hancock@hutton.ac.uk

Redox control of aphid resistance through altered cell wall composition and nutritional quality.

Brwa Rasool¹, Jack McGowan¹, Daria Pastok¹, Sue E. Marcus¹, Jenny A Morris², Susan R Verrall²; Peter E Hedley², Robert D Hancock^{2*}, Christine H Foyer^{1*}

¹Centre for Plant Sciences, School of Biology, Faculty of Biological Sciences, University of Leeds, LS2 9JT. United Kingdom.

²Cell & Molecular Sciences, The James Hutton Institute, Invergowrie, Dundee DD2 5DA

One sentence summary: Low ascorbate oxidase activities lead to a more reduced apoplastic redox state and enhance aphid resistance through changes in cell wall composition and decreased leaf nutritional quality.

Key words: antioxidants, (1-4)- β -D-galactan, homogalacturonan, nutritional quality, reactive oxygen species, RBOH

Abbreviations:

Figures: 6

Tables: 2

Supplementary Tables: 4

Supplementary Figures: 1

Footnotes

Author contributions: CHF conceived the study; CHF, RDH and PEH designed experiments; BR, JM, DP, SEM and JAM conducted experiments; SRV conducted statistical analysis; CHF and RDH wrote the manuscript with input from PEH.

Funding information: This work was supported by the Ministry of Higher Education and Scientific Research, Iraqi-Kurdistan Regional Government through the HCDP program (Brwa Rasool). The James Hutton Institute receives support from the Rural and Environment Science and Analytical Services Division of the Scottish Government. CHF thanks the Biotechnology and Biological Sciences Research Council (BBSRC) UK (BB/M009130/1) for financial support.

* **Corresponding authors:** Christine H. Foyer, C.Foyer@leeds.ac.uk; Robert D. Hancock, rob.hancock@hutton.ac.uk

ABSTRACT

The mechanisms underpinning plants perception of phloem feeding insects, particularly aphids, remain poorly characterized. The role of apoplastic redox state in controlling aphid infestation was therefore explored using transgenic tobacco plants that have either high (PAO) or low (TAO) ascorbate oxidase (AO) activities relative to the wild type. Only a small number of leaf transcripts and metabolites were changed in response to genotype and cell wall composition was largely unaffected. Aphid fecundity was significantly decreased in TAO plants compared to other lines. Leaf sugar levels were increased and maximum extractable AO activities were decreased in response to aphids in all genotypes. Transcripts encoding the Respiratory Burst Oxidase Homologue F, signaling components involved in ethylene and other hormone-mediated pathways, photosynthetic electron transport components, sugar, amino acid and cell wall metabolism were significantly increased in the TAO plants in response to aphid perception relative to other lines. The levels of galactosylated xyloglucan were significantly decreased in response to aphid feeding in all the lines, the effect being the least in the TAO plants. Similarly, all lines exhibited an increase in tightly bound (1→4)- β -galactan. Taken together, these findings identify AO-dependent mechanisms that limit aphid infestation.

INTRODUCTION

Phloem-feeding insects, of which aphids are the largest group, are major pests of crops and garden plants alike. Aphids navigate their feeding stylets through the plant tissues in order to access the sugars and amino acids in the sieve elements that form their food supply (Will and van Bel, 2006). During the feeding process, aphids unwittingly act as vectors for disease-causing viruses (Tjallingii, 2006). Aphids obtain nutrients directly from the phloem sap of the host plant secreting two types of saliva along the feeding tract of the chitinous stylet, which passes between the primary and secondary cell wall layers, making use of the large radial intercellular spaces, wherever possible. The gelling or sheath saliva not only stabilizes the stylet, allowing better movement through the cell walls but may also help the aphid avoid detection by preventing direct contact between the stylet and the plant cells. This saliva contains a mixture of enzymes such as pectinases, cellulases, phenol oxidases and peroxidases, which appear to function in cell wall breakdown. While the progress of the stylets through the host cell walls is considered to be too fast to allow significant metabolism by these the enzymes, the presence of these activities will undoubtedly contribute to the generation of signals that alert the host cells to the presence of the herbivore. Moreover, these and other proteins in saliva are considered to function as effectors that manipulate host cell processes and promote infestation (Jaouannet et al., 2014).

The “watery saliva”, which is produced after sheath-salivation, prevents the plant wound responses that might otherwise block and repair stylet probing points (Will et al., 2009). One such response is the production of callose outside the plasma membrane around plasmodesmata, effectively closing the pores linking the phloem sieve tubes (Will and van Bel, 2006). However, other than callose production, the functional importance of cell wall degradation and modifications has hardly been considered in relation to effective plant resistance mechanisms against aphids. However, a bioinformatics analysis of data concerning phloem feeding insect-associated molecular patterns revealed that large numbers of transcripts associated with cell wall metabolism are significantly altered in response to phloem-feeding insects (Foyer et al., 2015). In particular, this analysis highlighted the importance of wall associated kinases and receptor-like kinases, particularly those containing the domain of unknown function (DUF) 26 (Foyer et al., 2015). Similarities between plant–aphid and plant–pathogen interactions have been suggested by demonstration of the involvement of plant resistance factors such as the NB-LRR domain finality proteins and the BRASSINOSTERIOD INSENSITIVE 1-ASSOCIATED RECEPTOR KINASE 1 (BAK1) in

plant responses to aphids (Bos et al., 2010a; Jaouannet et al., 2014; Prince et al., 2014). The perception of environmental threats results in the production of an oxidative burst that involves the generation of reactive oxygen species (ROS) in the apoplast (Bos et al., 2010a,b; Jaouannet et al., 2014). Increasing literature evidence suggests that aphid-induced increases in ROS levels, together with the differential expression of genes involved in ROS generation and responses to oxidative stress, are important in the plant response to aphids and to other phloem-feeding insects (Moloi and van derWesthuizen, 2006; Kerchev, et al., 2012a, b; Mai, et al., 2013; Liang et al., 2013; Borowiak-Sobkowiak et al., 2016).

The plasmalemma functions as a dynamic interface between the cell and the outside world, with the highly reduced cytoplasm on one face of the membrane and the relatively oxidized apoplast/cell wall compartment on the other (Noctor and Foyer, 2016). The apoplastic compartment is more oxidized than many of the intracellular compartments because it is largely devoid of antioxidants except for ascorbic acid (Vanacker et al., 2000; Pignocchi and Foyer, 2003). The highly oxidizing environment of the apoplast is important for cell wall growth and dynamics, which require the generation of strong oxidants such as the hydroxyl radical (Müller et al., 2009; Karkonen and Kuchitsu, 2015). Ascorbic acid, which is the most abundant low molecular weight antioxidant in the apoplast, is a co-substrate for enzymes involved in cell wall stiffening, including peptidyl-prolyl-4 hydroxylase, which catalyzes the hydroxylation of proline residues of cell wall-associated hydroxyproline-rich glycoproteins (HRGPs), such as extensins and arabinogalactan proteins. Mutants that are impaired in ascorbate synthesis and thus have lower total leaf ascorbate levels have a higher resistance to aphid infestation because of priming of oxidative signaling pathways, such as the ABI4-dependent pathway (Pastori et al., 2003; Kerchev et al., 2013).

ROS production in the apoplast is catalyzed by a range of enzymes including members of the NADPH oxidase family that are also called Respiratory Burst Oxidase Homologues (RBOH)s, peroxidases, oxalate oxidases and other pro-oxidant enzymes. Apoplastic hydrogen peroxide has been shown to exert a strong influence on phenolic metabolism in Norway spruce cell cultures and to modify lignin formation and polymerization (Laitinen et al., 2017). The ROS burst that occurs upon perception of a physical or chemical signal triggers redox signaling pathways that regulate plant growth as well as defense (Mittler et al., 2011; Foyer et al., 2017; Kimura et al., 2017; Tang et al., 2017). ROS signaling transmits information locally through plasma membrane receptor-like kinases that modify metabolism

and gene expression, and systemically through processes called systemic acquired resistance and systemic acquired acclimation on environmental stress (Kimura et al., 2017; Tang et al., 2017; Mittler et al., 2012). Since the apoplast has few antioxidants, ROS are likely to have a longer lifetime in this compartment than they would have inside the cell (Pignocchi and Foyer, 2003; Parsons and Fry, 2012; Noctor and Foyer, 2016). While the roles of ROS in the apoplast have been extensively studied in relation to fungal and bacterial pathogens (Mittler, 2017; Kimura et al., 2017) relatively little is known about the roles of apoplastic ascorbate and ascorbate oxidase (AO) in this process (Pignocchi et al., 2016). Moreover, relatively few studies have concerned the role of oxidation of the apoplast on the plant response to aphid infestation.

AO is an apoplastic enzyme that catalyzes the first step of the ascorbate degradation pathway, oxidizing ascorbate to metabolites such as threonate and oxalate (Green and Fry, 2005; Parsons and Fry, 2012). In the following studies, the level of oxidation of the apoplast was changed by altering the level of AO and hence the availability of ascorbate in the apoplast. Transgenic tobacco plants that either express a tobacco AO gene in the antisense (TAO) orientation and therefore have low AO activity or that express a pumpkin AO gene (PAO) and thus have high levels of AO compared to the wild type (Pignocchi et al., 2003; Karpinska et al., 2017) were used to determine whether apoplastic redox state plays a specific role in limiting infestation by the generalist aphid, *Myzus persicae*. We have previously shown that the differences in maximal extractable leaf AO activities in PAO and TAO leaves result in large changes in the ascorbate and DHA contents of the apoplast without having any significant effects on the total ascorbate pool of the whole leaf ascorbate or leaf ascorbate/DHA ratios (Pignocchi et al., 2003, Karpinska et al., 2017). Here we present data showing a strong interaction between AO activity and the degree of aphid fecundity and infestation. The maximal extractable activity of AO activity was decreased in response to aphid infestation in all lines. Moreover, aphid fecundity was highest when leaf AO activity was low and hence the apoplast was more reduced. Low AO activity decreases leaf oxalate levels and changed the composition of the cell wall, resulting in a decreased abundance of (1-4)- β -D-galactan and increased levels of methyl-esterified epitopes of homogalacturonan and pectic polysaccharides. In addition, leaves with low AO activity had significantly lower levels of many amino acids within hours of the onset of infestation compared to the other lines. Infected plants therefore respond to aphid attack by decreasing leaf apoplastic AO

activity, a mechanism that decreases the nutritional quality of the leaves and may serve to impair aphid feeding by alterations in the structure of the cell wall.

RESULTS

Shoot phenotypes were similar in all lines when plants were grown for 8 weeks under controlled environment conditions. At this stage, all plants had a similar number of leaves with a similar shoot biomass accumulation and the same leaf pigment content and composition, such i.e. in terms of chlorophyll and carotenoids (data not shown). There were no significant differences in these parameters between aphid-free and aphid-infested plants i.e. where a single aphid was added to each plant at the 6-week old growth stage (data not shown).

Reciprocal interactions between leaf AO activity and aphid fecundity

Aphid fecundity was determined on 6 week old plants by placing a single one-day old nymph onto individual tobacco plants and counting the total number of aphids present on each plant after 14 days. Aphid fecundity was significantly reduced on TAO leaves relative to PAO leaves with an average of 19 aphids per plant on the former and 39 on the latter (Fig. 1). Aphid fecundity was intermediate on WT plants with an average of 26 aphids per plant. However, this value was not significantly different from either of the transgenic lines as estimated by one-way ANOVA ($p < 0.05$).

Maximal extractable AO activities were measured in the leaves of 8 week-old plants that had either been grown in the absence of aphids throughout the vegetative growth period or with aphid infestation from 6 weeks, as described above (Figure 2A). The PAO leaves had the highest extractable AO activities in the absence or presence of aphids compared to the WT and TAO leaves (Fig. 2A). Leaf AO activity was decreased by approximately 55% as a result of aphid infestation in all the lines ($P < 0.05$), as determined by two-way analysis of variance (Fig. 2A). Subsequent one-way analysis of variance treating each genotype-infestation combination as a single factor indicated that reduced AO activity following infestation was only significant in the PAO lines although the same trend was observed in all lines. Furthermore when AO activity was plotted against aphid fecundity, there was a strong linear correlation ($R^2 = 0.97$) between aphid fecundity and AO activity in the infested plants (Fig. 2B). Hence, AO activity has a strong impact on aphid fecundity.

AO activity and aphid infestation-dependent changes in the leaf transcriptome

To understand mechanisms underlying differential aphid resistance between lines with different levels of AO activity, we conducted an analysis of the leaf transcript profiles of WT, antisense TAO and sense PAO leaves that were either aphid-free or had been infested with aphids for 12 h. We chose this time point because it was within the range of the early transcriptome responses to aphid infestation that have been reported previously (Foyer et al., 2015). A two-way analysis of variance was used to identify transcripts that were significantly altered in abundance in relation to genotype or as a result of aphid infestation. Only a relatively small number of transcripts (132) showed differential regulation with regard to genotype, in agreement with our previous report (Karpinska et al., 2017; Table S1). In contrast, aphid infestation had a greater influence on the leaf transcriptome, with more than 1100 transcripts exhibiting significantly different abundance in response to aphid infestation (Table S2).

To refine the lists of differentially abundant transcripts further, any transcripts that exhibited a fold change of less two between aphid-free and infested plants in one or more genotypes were removed from subsequent analysis. This left a total of 501 transcripts that had a greater than two fold increase in abundance and 68 transcripts that were more than two fold less abundant in one or more lines following aphid infestation (Fig. 3). To identify transcripts that were associated with differing degrees of aphid resistance between lines, we identified transcripts that were specifically highly induced or repressed in specific lines. This analysis revealed that the TAO plants with low AO activity, which were more resistant to aphids than the other tobacco lines, exhibited unique accumulation of 252 transcripts and unique depletion of 16 transcripts (Fig. 3). In contrast, PAO lines that were the most aphid susceptible lines uniquely accumulated only 17 transcripts that was matched by the number of transcripts that were uniquely depleted (Fig. 3). The differences in transcript abundance were confirmed by qPCR (Figure S1).

An analysis of hormone-related transcripts suggests that aphid infestation in the TAO plants resulted in increased ethylene synthesis and signaling, resulting from significant increases in the abundance of transcripts encoding proteins with homology to 1-aminocyclopropane-1-carboxylate oxidase, several ethylene responsive proteins and a number of AP2/ETHYLENE RESPONSE ELEMENT BINDING PROTEIN transcription factors (Fig. 4; Table S3). The increased abundance of transcripts associated with ethylene synthesis and signaling is a common response of *Arabidopsis* to infestation by aphids (Foyer et al., 2015). The data

suggest that a similar response is observed in the tobacco leaves with low levels of AO activity and hence, a more reduced apoplast. Other hormone-related transcripts indicate roles for ABA, auxin, and jasmonate in the increased resistance response observed in the TAO plants (Fig. 4; Table S3). Furthermore, a transcript with homology to the Arabidopsis *MYC2* transcription factor was significantly increased only in the TAO plants. Along with *MYC3* and *MYC4*, *MYC2* is a target for JAZ repressors and plays a key role in orchestrating SA/JA crosstalk in response to the perception of insect attack (Schmiesing et al., 2016). A transcript with homology to *WRKY40* was also highly expressed in TAO leaves in response to aphid infestation. An increased abundance of this transcription factor is a common feature of the Arabidopsis – aphid interaction where it plays a role in the coordination of SA/JA/ABA signaling (Foyer et al., 2015).

In addition to hormone-related pathways, several transcripts that are associated with other key signaling pathways and that have been implicated in insect perception and signal transduction previously, were specifically increased only in the TAO plants. For example, a transcript with homology to *RBOHF* was much more abundant in TAO leaves compared to the WT and PAO lines (Fig. 4, Table S3). Previous work has demonstrated the requirement of an RBOH propagated ROS wave in systemic signaling following aphid infestation (Miller et al., 2009; Mittler et al., 2011). Similarly, a transcript encoding a protein with homology to a glutamate like receptor protein was specifically highly expressed in TAO leaves following aphid infestation. The proteins encoded by these transcripts have previously been demonstrated to transmit long distance wound induced signals and are required for systemic jasmonate accumulation (Mousavi et al., 2013).

A key difference between the transcript profiles in the TAO and PAO plants was the response of transcripts associated with photosynthesis to aphid infestation. For example, transcripts associated with cyclic electron flow were increased in abundance in the TAO leaves. In contrast, transcripts encoding chlorophyll a/b-binding proteins were much more abundant as a result of infestation by aphids only in PAO plants (Table S3). Changes in photosynthetic gene expression are an almost universal plant response to insect attack (Kerchev et al., 2012a) however little is known regarding how specific changes may influence plant-insect interactions. The data presented here suggest that the redox state of the apoplast exerts an influence over photosynthetic gene expression in response to aphid perception, as has been observed in response to light (Karpinska et al., 2017).

A number of transcripts associated with putative defense functions were highly increased in abundance following aphid infestation only in the TAO lines. For example several transcripts encoding structural phloem proteins were more abundant in TAO lines than other lines following aphid infestation (Fig. 4, Table S3). These proteins are believed to have a role in sieve element occlusion which might impede aphid feeding although this widely accepted view has more recently been challenged (Knoblauch et al., 2014). Several transcripts associated with cell wall metabolism and re-modeling were greatly increased in TAO lines but were not significantly changed in other lines in response to aphid infestation (Fig. 4, Table S3). We previously observed that changes in transcripts indicative of a potential re-modeling of the cell wall were a common response of Arabidopsis plants to aphid infestation (Foyer et al., 2015). We therefore conducted further analysis of changes in plant cell wall epitopes as described below.

Sense PAO plants have a low leaf amino acid phenotype but leaf amino acids are less responsive to aphid infestation than in antisense TAO or WT plants

To obtain further insight into the resistance mechanisms operating in the TAO plants to limit *M. persicae* infestation, we conducted GC/MS metabolite profiling analyses of the TAO, WT and PAO plants either in the absence of aphids or following 12h aphid infestation. Nine metabolites were significantly changed in abundance with respect to genotype in the tobacco leaves. Twenty metabolites exhibited an altered abundance as a result of aphid infestation and a further ten metabolites were significantly altered in abundance following infestation in a genotype-specific manner (Table S4).

A key observation was that while PAO leaves had lower levels of many amino acids compared to the TAO or WT leaves in the absence of aphids, the amino acid profile of the PAO leaves was less responsive to aphid infestation than the other genotypes (Fig. 5, Table S4). In contrast, the amino acid profiles of both the WT and TAO leaves were highly responsive to aphids, having significantly lower levels of many amino acids 12 h after infestation compared to aphid-free controls. Indeed, TAO leaves appeared to be hypersensitive to aphids in terms of amino acid responses, having lower amino acid levels than the infested WT or PAO leaves. Interestingly, all genotypes exhibited large increases in the contents of free sugars and sugar alcohols in the leaves following exposure to aphids (Fig.

5, Table S4). These data indicate that one potential mechanism of aphid resistance is to limit the nutritional quality of leaves by reducing the availability of limiting amino acids and increasing the osmotic pressure of the phloem.

AO activity and aphid infestation alter cell wall composition

The relative composition of the cell wall was determined in the different lines in the absence or presence of aphids by ELISA using specific antibodies that recognise the range of cell wall components listed in Table 1. A two-way analysis of variance for each of the fractions and each of the antibodies was performed using the factors aphid infestation and genotype (Table 2). In the absence of aphids, the leaves of the all the tobacco lines had a very similar cell wall composition regardless of AO activity (Figure 6A, C, E) as illustrated by the lack of significant changes in abundance of any of the epitopes based upon the factor genotype in the analysis of variance (Table 2). However, following aphid infestation several significant differences in the cell wall composition between the genotypes were observed (Figure 6B, D, F; Table 2). Levels of galactosylated xyloglucan recognised by LM25 were significantly altered in all fractions (water extract, CDTA extract and KOH extract) following infestation by aphids (Fig. 6, Table 2). There was a clear reduction in the levels of xyloglucan in the KOH extractable cell wall fraction from all genotypes although this was less marked in the TAO leaves compared to the effect in other genotypes (Fig. 6). Moreover, the relative abundance of RG-1 related (1→4)- β -galactan (recognised by LM5) was significantly higher in the KOH fraction of all genotypes following aphid infestation (Fig. 6, Table 2).

DISCUSSION

The cell wall represents a first line of defense for plant cells against the penetration of the aphid feeding stylet and hence the ability of these phloem-feeding insects to gain the nutrients that they require to support growth and reproduction. It has long been recognized that herbivores can be deterred from feeding by changes in cell wall thickness as a result of lignification and suberization (War et al., 2012). However, while the oxidative burst in the apoplast is a common feature of plant responses to pathogens and herbivory, aphid-triggered changes in cell wall composition have not previously been described in detail. The data presented here not only provide the first evidence that cell wall composition can be modified in response to herbivory to limit infestation but also demonstrates that AO and the redox state of the apoplast plays a key role in this process. The data presented here demonstrate that the responses of tobacco leaves to aphid attack are influenced by the level of leaf AO. It is interesting to note that maximum extractable AO activities were decreased by aphid infestation in all genotypes, not least because aphid fecundity was the most restricted in plants where AO activity was lowest. It is unlikely that this response is caused by altered expression in the PAO plants. Hence, this finding suggests that aphid-induced decreases in AO activity are achieved via post-transcriptional mechanisms.

The redox environment of the apoplast is highly dynamic because it does not contain the range or levels of low molecular weight antioxidants available in the cytoplasm (Munné-Bosch et al., 2013). Discrete changes in the ascorbate/DHA ratios of the apoplast/cell wall compartment were facilitated by alterations in the levels of AO activity without any significant effects on the whole leaf ascorbate pool, as shown previously (Pignocchi et al., 2003; 2006; Karpinska et al., 2017). The relative abundance of a small number of leaf transcripts such as those involved in amino acid metabolism and metabolites such as oxalate were changed in response to changes in AO activity. However, cell wall composition was largely unaffected by changes in AO activity alone. Crucially, the plant response to aphid perception was to lower AO activity in all lines. Moreover, the level of AO activity in the transgenic lines had a strong influence on aphid fecundity, plants with low AO activity having a greater ability to restrict aphid infestation than other lines.

AO activity and hence the redox state of the apoplast exerted a strong influence on the extent of the plant response to aphid infestation in terms of altered cell wall composition. The

perception of aphids decreased the relative abundance of galactosylated xyloglucan in the cell wall in all lines, regardless of AO activity. However, the decrease in the relative abundance of xyloglucan was less marked in the TAO leaves that have high ascorbate/DHA ratios, i.e. where the apoplast is in a more reduced state. Moreover, the levels of (1→4)-β-galactan were significantly elevated in all lines following aphid infestation. These data suggest that changes in cell wall composition, particularly with regard to epitopes of rhamnogalacturonan-I and xyloglucans are associated with aphid infestation of tobacco leaves. The observation that the most resistant line with respect to infestation (TAO) exhibited the least alteration in xyloglucan epitope abundance may imply that the observed changes in cell wall composition might facilitate aphid feeding. Changes in the composition of the cell wall of the type described here could reflect alterations in cell wall growth. For example, the transient occurrence of a pectic (1→4)-β-D-galactan epitope in cell walls was found to precede the main phase of cell elongation in *Arabidopsis* roots (McCartney et al., 2003). Pectic polysaccharides form a cross-linked three-dimensional hydrated network that provides a suitable environment to regulate the access or activities of cell wall-modifying proteins.

Homogalacturonan, rhamnogalacturonan-I and rhamnogalacturonan-II are major pectic polymers but their precise functions are largely unknown. Homogalacturans, which are the most abundant pectic polymers, are involved in the formation of calcium cross-linked gels (Jones et al, 1997). Changes in the abundance of these pectic polymers may therefore exert an important influence over cell wall structure, particularly the properties of the cellulose–hemicellulose network. The data presented here show that high levels of AO limits the capacity of infested leaves to make these aphid defence-appropriate changes to cell wall composition. High AO activities resulting in a more oxidised apoplast may favour an increased generation of hydroxyl radicals within the walls. This may not be beneficial because it would provoke the cleavage of cell wall sugars, leading to cell wall loosening (Müller et al., 2009). Cell wall loosening is likely to aid the passage of the chitinous aphid stylet between the primary and secondary cell wall layers. Conversely, an enhanced oxidation of the apoplast may result in cross-linking of phenolic acids in the cell wall resulting in stiffening and an inhibition of growth (Lu et al., 2014). However, the high AO activity in the PAO lines alone does not alter plant growth and development (Pignocchi et al., 2003). Moreover, the high levels of ascorbate in the apoplast in the TAO plants would favor

strengthening of the wall because of the requirement of this substrate in reactions catalyzed by peptidyl-prolyl-4 hydroxylases.

Changes in the cell wall architecture activate signaling pathways connected with cellular expansion, growth inhibition and programmed cell death (Tenhaken, 2015). Redox changes in the apoplast are likely to influence a wide range of cell wall processing enzymes that have *N*-glycosylation sites, cysteine thiols and disulfide bonds. Post translational modifications of these enzyme proteins protects them from proteolytic degradation and provides accurate targeting of *N*-glycoproteins (Zielinska et al., 2012; Ruíz-May et al., 2014). While callose can be deposited in the cell wall around the plasmodesmata to plug the sieve plates and deter feeding (Will & van Bel, 2006), no significant changes in the expression of callose synthases or endo-1,3- β -glucanases were observed in the present studies. This observation suggests that callose is not that important in the responses of tobacco plants to aphid infestation. Although callose deposition is a common feature of plant defenses to fungal and microbial pathogens, its precise functions in many plant defense responses remain unclear. While, for example, the *Arabidopsis pmr4-1*, which lacks callose synthase, was identified on the basis of its enhanced resistance to powdery mildew (Nishimura et al., 2003), papillae are still produced in the mutant similar to the wild type plant (Soylu et al., 2005).

A relatively small number of transcripts showed differential regulation with regard to genotype. We have discussed the details of the transcript changes related to AO activity previously (Karpinska et al., 2017; Table S1), and so we will not discuss these features in detail here, except to mention that RBOHF and a calcium channel protein associated with plant defenses to fungal pathogens was differentially expressed in relation to AO activity (Pignocchi et al., 2006). We have previously shown that while the leaves of the PAO lines show constitutive activation of the MAPK signaling coupled to the decreased expression of the calcium channel NtTPC1B, which encodes a voltage-operated calcium channel that is activated by hydrogen peroxide, the TAO lines lower expression showed increased resistance to a virulent strain of *Pseudomonas syringae* (Pignocchi et al., 2006). This finding is consistent with the enhanced resistance to aphids observed in the present studies. A recent study in maize has shown that enhanced expression of all RBOH genes was observed in cultivars that were more resistant to the bird cherry-oat aphid (*Rhopalosiphum padi* L.) compared to susceptible lines (Sytykiewicz 2016). RBOHF fulfils a diverse range of

functions in plants including pathogen responses and abiotic stress signaling, lignification and stomatal closure (Suzuki *et al.*, 2011; Chaouch *et al.*, 2012). The significantly increases in *RBOHF* transcripts observed in the TAO leaves in response to aphid perception is consistent with the increased level of resistance to aphid infestation observed in plants with low AO activity.

Analysis of the transcriptome profiles of leaves reveals that aphid feeding in plants with a more reduced apoplastic state triggered synergistic effects among different components of the plant defensive system. Transcripts that were uniquely highly increased in abundance in plants with low AO activity may provide novel insights into the signaling and resistance mechanisms associated with enhanced resistance to aphid infestation. The TAO leaves that have low AO activity showed an increased abundance of subsets of transcripts suggesting enhanced signaling through ethylene and SA/JA/ABA-dependent pathways that are important in limiting invasion by these herbivores (Foyer *et al.*, 2015) compared to the other lines. In addition, analysis of the leaf metabolite profiles revealed aphid-induced changes in the partitioning of carbon between sugars and amino acids in the leaves of the WT and TAO leaves. While large increases in leaf free sugars and sugar alcohols was observed in all genotypes following exposure to aphids, significantly lower levels of many amino acids were found only in the leaves of the WT and TAO lines compared to aphid-free controls.

The data presented here show that plants respond to aphid perception by metabolic triage that limits the nutritional quality of leaves, a process that may be key to limiting aphid fecundity. Crucially, the ability of the plants to limit the availability of major amino acids is strongly influenced by the redox state of the apoplast. It has previously been shown that low AO activities in tomato not only increased leaf sugar contents but also altered apoplastic hexose:sucrose ratios (Garchery *et al.*, 2013). It is therefore likely that the sugar and amino acid composition of the phloem is changed as a result of the low AO activities in tobacco leaves studied here, and that this contributes to the limitation of infestation. However, it is important to note that the action of AO gene products may extend beyond effects exerted through direct changes in AO activity. For example, expression of the rice AO protein, OsORAP1, which is localized in the apoplast but has no AO activity, enhances cell death in leaves exposed to ozone or pathogens (Ueda *et al.*, 2015). OsORAP1, whose expression was highest in photosynthetic tissues with the highest stomatal conductance, influences jasmonic acid pathway signalling to mitigate ozone symptoms by unknown mechanisms (Ueda *et al.*, 2015).

In conclusion, these data extend our current understanding of plant responses to aphids, which cause significant losses to crop production and also devastate garden plants. In particular, these findings contribute to our knowledge of how plants limit infestation by some of the most economically-important aphid species, which have exceptionally broad host ranges, such as *M. persicae*. Taken together, the findings reported here show that AO and the redox properties of the apoplast fulfil important roles in limiting aphid infestation. In the absence of the perception of the biotic threat changes in leaf AO levels had relatively little effect on the leaf metabolome or transcriptome. However, low leaf AO activities that allow the redox state of the apoplast to be more reduced, enhance the aphid-induced defense responses in terms of changes in (a) cell wall composition (b) the leaf metabolite profile, particularly in terms of amino acids and sugars, and (c) the leaf transcript profile, specifically changing sub-sets of transcripts encoding proteins involved in hormone-mediated defense pathways. Taken together, these data provide a better understanding of the molecular basis for plant–aphid interactions.

ACKNOWLEDGEMENTS

We are extremely grateful to Professor Paul Knox, who provided expert knowledge, guidance and a critical evaluation of the cell wall composition data.

METHOD AND MATERIALS

Plant material and growth conditions

The generation of transgenic tobacco (*Nicotiana tabacum* L.; T3 generation) lines expressing a pumpkin (*Cucurbita maxima*) ascorbate oxidase (AO) gene in the sense orientation (GenBank accession number X55779) or a partial tobacco AO sequence in the antisense orientation (GenBank accession number D43624) has been described previously (Pignocchi et al., 2003; 2006). Plants were grown in compost (SHL professional potting compost) under an 8h/16h day/night regime with an irradiance of 250 $\mu\text{mol m}^{-2} \text{s}^{-1}$. The relative humidity was 60% and temperature was maintained at a constant 20°C. Seeds were sown in pots and allowed to germinate and grow for a week before seedlings were transferred to individual pots and allowed to grow for a further 5 weeks prior to aphid infestation experiments.

Aphid material and culture conditions

Apterous *Myzus persicae* clone G (Kasprowicz et al., 2008) were maintained on wild type tobacco plants in transparent Perspex cages with 16h/8h day/night periods.

Aphid infestation and reproductive performance

After 6 weeks growing under controlled environments as described wild-type (WT), antisense tobacco ascorbate oxidase (TAO) and sense pumpkin ascorbate oxidase (PAO) plants were transferred to individual plastic containers sealed with mesh lids. Plants were infested with a single 1 day old *M. persicae* nymph and the aphid colony maintained for 14 days prior to counting as previously described (Kerchev et al., 2012b). Each experiment involved 6 plants per line and each experiment was repeated between 3 and 6 times.

To determine the effect of aphids on the leaf transcriptome, six 6 week old plants per line were infested by transfer of 60 adult apterous aphids to the adaxial surface of the youngest fully mature leaf. Aphids were then confined in a 2.5 cm diameter clip cage comprising a 200 μm mesh size for 12 h. Control plants were fitted with the clip cage but were not infested. Following infestation, aphids were quickly removed from the infested leaf which was then rapidly frozen in liquid nitrogen prior to RNA extraction and microarray processing

as described below. Each of the three biological replicates per line consisted of two leaves from different plants.

Ascorbate Oxidase Activity

The youngest fully expanded leaves were harvested from three independent 4-week-old tobacco plants per genotype per time point as described above and immediately frozen in liquid nitrogen. Frozen leaf tissue was ground to a fine powder, 0.1 M sodium phosphate buffer (pH 6.5) was added at a ratio of 10 ml g⁻¹ fresh weight and the mixture was ground until the buffer thawed. The extract was centrifuged for 10 min at 15000g and 4°C. The supernatant was discarded and the pellet was re-suspended in 0.1 M sodium phosphate (pH 6.5) containing 1 M NaCl. Insoluble material was pelleted again by centrifugation (10 min, 15000g, 4°C) leaving proteins ionically bound to the cell wall fraction in the supernatant. Maximal extractable ascorbate oxidase activity was estimated at 25°C as described by Pignocchi et al. (2003), via the decrease in absorbance at 265 nm following the addition of 50 µl of extract in a reaction mixture containing 0.1 M sodium phosphate (pH 5.6), 0.5 mM EDTA and 100 µM ascorbate. One unit of ascorbate oxidase activity is defined as the amount of enzyme required to oxidise of 1 µmol ascorbate min⁻¹.

Crude Cell Wall Preparation

Cell walls were prepared as alcohol insoluble residues (AIR) using a modification of the procedure described by Leroux et al. (2015). Leaf samples were lyophilised and ground in a bead beater at 50Hz for 2 min. Samples were then sequentially extracted in an aqueous ethanol series (70%, 80%, 90% and 100%) each for a period of one hour at room temperature. Samples were then extracted for 1 h in acetone prior to a final extraction in methanol/chloroform (2/3 v/v). Following the final extraction, the supernatant was removed and the insoluble residue left to dry overnight in a fume hood at room temperature.

Cell Wall Extraction

Cell wall polymers were sequentially extracted from AIR in a modification of the procedure described by Leroux et al. (2015). 1 mg AIR was weighed into a plastic tube, beads were added and the tube and content cooled in liquid N₂. The sample was then placed on a bead beater and ground at 50Hz for 2 minutes. 400µl of water was added and the tubes were

placed back onto the bead beater for 20 minutes at 50Hz. Tubes were then centrifuged at 14,000 g for 15 minutes and the supernatant collected as the water extractable fraction containing weakly bound pectins. 400µl of 50mM 1,2-cyclohexylenedinitrilotetraacetic acid (CDTA) was added to the pellet and extraction continued at 50 Hz for a further 20 minutes, the collected supernatant was considered the CDTA extractable fraction containing strongly bound pectins. Finally the pellet was resuspended in 400µl of 4M KOH containing 0.1% (v/v) NaBH₄ and the extraction repeated for 20 mins to collect the KOH soluble fraction comprising hemicelluloses. The KOH soluble fraction was neutralised with 80% acetic acid until a neutral pH was achieved.

Quantification of Cell Wall Epitopes

Cell wall epitopes in the different AIR fractions were estimated in triplicate using an enzyme-linked immunoabsorbent assay with the primary monoclonal antibodies listed in table 1. All antibodies are available from Plant Probes (www.plantprobes.net). Initial experiments were conducted to optimise extract dilution and subsequently AIR extracts were diluted 125-fold in phosphate-buffered saline (PBS). 100µl aliquots were loaded into 96-well polystyrene microplates (Nunc Immuno Plate, Thermo Scientific) and left to incubate overnight at 4°C. The following day plates were washed three times in tap water and then blocked for 1 h at room temperature with 200µl of 5% skimmed milk powder /PBS. Plates were again washed nine times with tap water and then dried. Primary antibody as supplied was diluted 10-fold in 5% skimmed milk powder in PBS and 100 µl added to microplate wells. Incubation was continued for 1h at room temperature then plates were washed nine times in tap water prior to drying. The secondary antibody goat anti-Rat IgG-HRP (Sigma) was diluted 1 in 1000 in 5% milk powder in PBS and 100ul added to each well prior to incubation at room temperature for 1h. Plates were again washed x9 and dried. To quantify antibody binding, a substrate was prepared comprising 1% (v/v) tetramethylbenzidine (10mg/ml) and 0.006% (v/v) H₂O₂ (6%) in 100 mM sodium acetate buffer pH 6.0 and 100µl was added to each well. The reaction was incubated at room temperature for 5 min and then stopped by addition of 50µl of 2.5M sulphuric acid. The absorbance at 450 nm was measured using a FLUROstar Omega BMG lab tech microplate reader.

RNA Extraction, microarray processing and analysis

Microarray experiments were conducted to compare gene expression in fully expanded leaves of tobacco genotypes (wild-type, antisense TAO and sense PAO) either infested with aphids for 12 h or in uninfested leaves as described under the aphid infestation and reproductive performance section above. . Three independent biological replicates were analysed for each condition and genotype and full experimental design and microarray datasets are available at ArrayExpress (<http://www.ebi.ac.uk/arrayexpress/>), accession E-MTAB-4816.

Microarray design ID 021113 (Agilent Technologies) was used with 43,803 probes representing tobacco transcript sequences. The One-Color Microarray-Based Gene Expression Analysis protocol (v. 6.5; Agilent Technologies) was used throughout for microarray processing. Briefly, cRNA was synthesized from cDNA which was then linearly amplified and labelled with Cy3 prior to purification. Labelled samples were hybridized to microarrays overnight at 65°C, prior to being washed once for 1 min with GE Wash 1 buffer (Agilent Technologies) at room temperature and once for 1 min with GE Wash Buffer 2 (Agilent Technologies) at 37°C, and then dried by centrifugation. The hybridized slides were scanned using the Agilent G2505B scanner at resolution of 5 µm at 532 nm.

Feature Extraction (FE) software (v. 10.7.3.1; Agilent Technologies) with default settings was used for data extraction from the image files. Subsequent data quality control, pre-processing and analyses were performed using GeneSpring GX (v. 7.3; Agilent Technologies) software. Agilent FE one-colour settings in GeneSpring were used to normalise data and a filter used to remove inconsistent probe data, flagged as present or marginal in less than 2 out of 18 samples. Two-way Analysis of Variance (ANOVA) using the factors aphid infestation and genotype was used to identify significant differentially expressed probes with a p-value ≤ 0.05 with Benjamini-Hochberg multiple testing correction.

Aphid dependent lists were further trimmed by removing any transcript that exhibited a less than two fold change in abundance between uninfested and infested conditions in at least one of the tobacco lines.

qPCR

Real time (qPCR) was performed on total RNA extracted from leaves using an Eppendorf Realplex2 real-time PCR system. One-step RT-PCR using Quantifast SYBR Green RT-PCR Kit (Qiagen) was performed according to the manufacturer's instructions. The expression of

the genes of interest was normalised using *A. thaliana* *UBIQUITIN 10* as an endogenous control. Each experiment, which involved 10 biological replicates per line, was repeated at least three times.

Metabolite profiling by GC/MS

GC/MS analysis was performed on extracts from three biological replicates per treatment essentially as described by Foito et al. (2013). The youngest fully expanded leaf was snap frozen in liquid nitrogen then lyophilized. 100 ± 5 mg of dried material were weighed into glass tubes and extracted in 3ml methanol for 30 minutes at 30°C with agitation (1500 rpm). 0.1 ml each of polar (ribitol 2 mg ml⁻¹) and non-polar (nonadecanoic acid methylester 0.2mg ml⁻¹) and 0.75ml distilled H₂O were added and extraction continued for a further 30 minutes as described. 6 ml chloroform were added and extraction continued for 30 minutes under increased agitation at 2500 rpm. Phase separation was achieved by the addition of a further 1.5 ml of water and centrifugation at 1000g for 10 minutes. Following oximation, polar metabolites were converted to trimethylsilyl derivatives while non-polar metabolites were subjected to methanolysis and trimethylsilylation as described (Foito et al., 2013). Metabolite profiles for the polar and non-polar fractions were acquired following separation of compounds on a DB5-MSTM column (15 m × 0.25 mm × 0.25 μm; J&W, Folsom, CA, USA) using a Thermo-Finnigan DSQII GC/MS system as described (Foito et al., 2013). Data was then processed using Xcalibur software. Peak areas relative to internal standard (response ratios) were calculated following normalization to 100 mg extracted material.

Accession numbers

Experimental design and microarray datasets are available at ArrayExpress (<http://www.ebi.ac.uk/arrayexpress/>), accession E-MTAB-4816.

TABLES

Table 1 List of antibodies used in this study

Target polymer ^a	mAb	Specificity	Reference
Pectic HG and related	JIM7	Partially methyl-esterified HG	Clausen <i>et al.</i> (2003)
	LM19	Partially or dimethyl-esterified HG	Verhertbruggen <i>et al.</i> (2009)
	LM20	Methyl-esterified HG	Verhertbruggen <i>et al.</i> (2009)
RG-1 related	LM5	(1→4)-β-galactan	Jones <i>et al.</i> (1997)
Hemicelluloses/XG	LM25	Galactosylated xyloglucan	Pedersen <i>et al.</i> (2012)
	LM28	Glucuronosyl substituted xylans	Cornuault <i>et al.</i> (2015)
Hemicelluloses/mannan	LM21	Heteromannan	Marcus <i>et al.</i> (2010)

^a HG, homogalacturonan; RG-I, rhamnogalacturonan-I; XG, xyloglucan

Table 2 Significance values of antibody binding to tobacco cell wall fractions from antisense PAO, WT and sense PAO lines grown in the absence or presence of aphids

Factor	Antibody						
	JIM7	LM19	LM20	LM21	LM5	LM25	LM28
<i>H₂O soluble fraction</i>							
Aphid	0.068	0.967	0.854	0.131	0.125	0.001	0.681
Genotype	0.391	0.148	0.161	0.901	0.757	0.051	0.853
Interaction	0.211	0.587	0.912	0.200	0.352	0.018	0.376
<i>CDTA soluble fraction</i>							
Aphid	0.089	0.508	0.415	0.907	0.177	0.023	0.874
Genotype	0.515	0.217	0.644	0.761	0.827	0.839	0.514
Interaction	0.310	0.431	0.658	0.366	0.224	0.155	0.867
<i>KOH soluble fraction</i>							
Aphid	0.992	0.116	0.783	0.192	0.018	0.001	0.694
Genotype	0.150	0.917	0.100	0.707	0.534	0.905	0.935
Interaction	0.167	0.314	0.237	0.083	0.736	0.026	0.137

Significance values were calculated for each cell wall fraction following two-way analysis of variance using the factors plant genotype and aphid infestation as well as any interacting effects. Values considered significant ($P < 0.05$) are highlighted in bold.

1. FIGURE LEGENDS

Figure 1 Impact of manipulation of ascorbate oxidase transcripts on aphid fecundity in tobacco.

Six week old WT, PAO and TAO plants were infested with a single 1 day old nymph of *Myzus persicae* and cultured for 14 days as described. The total number of aphids present after 14 days infestation is indicated as mean \pm SE (n =6). Different letters indicate significant differences between values as determined by one-way ANOVA and Fishers protected LSD test (P < 0.05).

Figure 2 Impact of aphid infestation on apoplastic ascorbate oxidase activity in tobacco leaves

WT, PAO and TAO tobacco plants were grown for six weeks in the absence of aphids. At the end of the six week period, one group of plants were infested with a single one-day old nymph while the remaining group were left in the absence of aphids and grown in cages for further two week as described. At the end of the two week period plants were harvested and apoplastic ascorbate oxidase activity quantified as described (A). Bars illustrate mean AO activity \pm SE (n = 6) and different letters above bars indicate values that were significantly different from one another according to Fishers protected LSD test. A linear relationship was observed between measured ascorbate oxidase activity and aphid fecundity (B).

Figure 3 Number of transcripts significantly altered in abundance in tobacco plants following infestation by *M. persicae*.

Significantly altered transcripts were identified by two way ANOVA (P<0.05) with Benjamini-Hochberg correction using the factors genotype and infestation. All transcripts that were significant for aphid infestation were selected and those that had a lower than two-fold differential abundance in any of the genotypes were discarded. The remaining transcripts were considered differentially abundant in any of the genotypes if they had a greater than two difference in abundance between infested and uninfested plants. Venn diagrams illustrate the number of transcripts significantly more (A) or less (B) abundant in TAO, WT and PAO lines as illustrated.

Figure 4 Heatmap of transcript abundance of key transcripts associated with signalling and defence following aphid infestation of antisense TAO, WT and sense PAO leaves.

Relative abundance of transcripts associated with hormone and other signalling pathways (A) or cell wall modification and defence (B) are illustrated according to the scale bar shown. Columns indicate transcript abundance in antisense TAO, wild-type and sense PAO in the absence (-) or presence (+) of aphids. Microarray probe identification numbers are indicated to the left of each row and a brief description of the gene product is provided to the right. Aux, auxin; CK, cytokinin; ET, ethylene; Aux GT, auxin glucosyltransferase; AOS, allene oxide synthase; GLR, glutamate-like receptor; ERF, ethylene response factor; NCED4, 9-cis-epoxycarotenoid dioxygenase 4; NAC TF, NAC domain transcription factor; RBOHF, respiratory burst oxidase homolog F; ACO, 1-aminocyclopropane-1-carboxylate oxidase; PP2, phloem protein 2; CES, cellulose synthase.

Figure 5 Influence of aphid infestation on leaf content of amino acids and sugars

Bar charts indicate the relative concentrations of amino acids and sugars significantly altered in abundance in leaves in response to aphid infestation and refer to antisense TAO, wild-type (WT) and sense PAO plants as indicated. Black bars indicate concentration in the absence of aphids and white bars in the presence of aphids and data are represented as mean \pm SE, n = 3. The figure indicates compartmentation and metabolic relationships between different compounds and presumed transporters are indicated as purple circles. 3-PGA, 3-phosphoglycerate; TP, triose phosphates; E4P, erythrose-4-phosphate; C5, five carbon Calvin pathway intermediates; PEP, phosphoenolpyruvate; Pyr, pyruvate; AcCoA, acetyl-coenzyme A; OAA, oxaloacetate; α -KG, α -ketoglutarate; GABA, γ -amino butyrate; Glc, glucose; Frc, fructose. Amino acids are indicated according to their standard 3 letter abbreviation.

Figure 6 Influence of aphid infestation on cell wall epitopes in tobacco leaves

TAO (A,B), wild-type (C,D) and PAO (E,F) plants were either grown in the absence (A, C, E) or presence (B, D, F) for 15 days prior to the preparation of cell walls as alcohol insoluble residues. Water (H₂O), CDTA and KOH extracts were prepared as described and the relative abundance of wall epitopes was estimated following probing with specific antibodies as shown. Different cell wall components were quantified by ELISA using the specific antibodies: JIM7, LM19, LM20, LM21, LM5, LM25 and LM28. Graphs show the relative quantitation determined using each antibody. Values were estimated as the absorbance measured in the linear range following incubation with HRP substrate divided the sum of absorbances.

SUPPLEMENTARY MATERIAL

Table S1 Transcripts exhibiting genotype dependent differences in relative abundance in antisense TAO, WT and sense PAO tobacco lines

Microarray experiments were conducted as described in infested and uninfested tobacco lines and transcripts with significantly altered abundance between samples were identified by two-way ANOVA with Benjami-Hochberg multiple testing correction. Transcripts that exhibited altered abundance dependent on genotype are indicated by their GenBank accession number (Primary accession) and the identification of the corresponding microarray probe is listed (Probe ID). The relative transcript abundance for uninfested and infested TAO, WT and PAO plants are provided and cells are highlighted according to a red (high relative abundance) to blue (low relative abundance) colour scale. The nearest Arabidopsis homologue is listed and the e-value of the match is provided as is a short description.

Table S2 Transcripts exhibiting aphid infestation dependent differences in relative abundance in antisense TAO, WT and sense PAO tobacco lines

Microarray experiments were conducted as described in infested and uninfested tobacco lines and transcripts with significantly altered abundance between samples were identified by two-way ANOVA with Benjami-Hochberg multiple testing correction. Transcripts that exhibited altered abundance dependent on aphid infestation are indicated by their GenBank accession number (Primary accession) and the identification of the corresponding microarray probe is listed (Probe ID). The relative transcript abundance for uninfested and infested TAO, WT and PAO plants are provided and cells are highlighted according to a red (high relative abundance) to blue (low relative abundance) colour scale. The nearest Arabidopsis homologue is listed and the e-value of the match is provided as is a short description.

Table S3 Transcripts uniquely altered in abundance by more than two fold following aphid infestation in antisense TAO, WT or sense PAO tobacco lines

Transcripts exhibiting a greater than two fold change in expression following aphid infestation uniquely in individual tobacco lines are indicated. Transcripts are sorted according to MapMan bin number and then microarray probe identification (Probe ID). A brief description of putative function is provided and the relative change in abundance

between uninfested and aphid infested plants is indicated. Fold change in expression is colour coded from red (high) to blue (low) for ease of reference.

Table S4 Influence of genotype and aphid infestation on metabolite content of tobacco leaves. Relative metabolite concentration was estimated in antisense TAO, wild type and sense PAO leaves either in the absence of aphids or following aphid infestation by GC/MS as described. Data was analysed by two-way ANOVA (genotype, aphids) and statistical significance (F. pr.) and standard errors of difference (s.e.d.) are indicated for each of the factors independently as well as their interaction and those that are statistically significant ($P < 0.05$) are indicated. Unknown non-polar (UNP) and polar (NP) metabolites are indicated by their retention time while fatty acids are indicated by their chain length and number of unsaturated bonds e.g. linoleic acid, C18:2. Fatty alcohols are indicated by their chain length followed by the abbreviation alc.

Figure S1 Comparison of microarray and qRT-PCR expression data. Relative transcript abundance was estimated using tobacco microarrays or qRT-PCR, as described in the materials and methods section. qRT-PCR data are presented as mean \pm SE, $n = 3$.

References

Borowiak-Sobkowiak B, Woźniak A, Bednarski W, Formela M, Samardakiewicz S, Morkunas I. (2016) *Brachycorynella asparagi* (Mordv.) induced-oxidative stress and antioxidative defenses of *Asparagus officinalis* L. *Int. J. Mol. Sci.* **17**: 1740.

Bos JIB, Prince DC, Pitino M, Maffei ME, Win J, Hogenhout SA (2010a) A functional genomics approach identifies candidate effectors from the aphid species *Myzus persicae* (Green Peach Aphid). *PLoS Genet.* **6**: e1001216

Bos JIB, Armstrong MR, Gilroy EM, Boevink PC, Hein I, Taylor RM, et al. (2010b) *Phytophthora infestans* effector AVR3a is essential for virulence and manipulates plant immunity by stabilizing host E3 ligase CMPG1. *Proc Natl Acad Sci U.S.A.* **107**: 9909–9914

Chaouch S, Queval G, Noctor G (2012) *AtRbohF* is a crucial modulator of defence associated metabolism and a key actor in the interplay between intracellular oxidative stress and pathogenesis responses in Arabidopsis. *Plant J.* **69**: 613–27.

Clausen MH, Willats WGT, Knox JP (2003) Synthetic methyl hexagalacturonate hapten inhibitors of anti-homogalacturonan monoclonal antibodies LM7, JIM5 and JIM7. *Carbohydr Res* **338**: 1797-1800.

Cornuault V, Buffetto F, Rydahl MG, Marcus SE, Torode TA, Xue J, Crépeau M-J, Faria-Blanc N, Willats WGT, Dupree P, Ralet M-C, Knox JP (2015) Monoclonal antibodies indicate low-abundance links between heteroxylan and other glycans of plant cell walls. *Planta* **242**: 1321-1334.

Foito A, Byrne SL, Hackett CA, Hancock RD, Stewart D, Barth S (2013) Short-term response in leaf metabolism of perennial ryegrass (*Lolium perenne*) to alterations in nitrogen supply. *Metabolomics* **9**: 145–156

Foyer CH, Ruban AV, Noctor G (2017) Viewing oxidative stress through the lens of oxidative signalling rather than damage. *Biochem. J.* **474**: 877–883

Foyer CH, Verrall SR, Hancock RD (2015) Systematic analysis of phloem-feeding insect induced transcriptional reprogramming in *Arabidopsis* highlights common features and reveals distinct responses to specialist and generalist insects. *J Exp Bot* **66**: 495–512

Garchery C, Gest N, Do PT, Alhag Dow M, Baldet P, Menard G, Rothan C, Massot C, Gautier H, Aarrouf J, Fernie AR, Stevens R (2012) A diminution in ascorbate oxidase activity affects carbon allocation and improves yield in tomato under water deficit. *Plant Cell Environ* **36**: 159-175

Green MA, Fry SC (2005) Vitamin C degradation in plant cells via enzymatic hydrolysis of 4-O-oxalyl-L-threonate. *Nature* **433**: 83–87

Jaouannet M, Rodriguez PA, Thorpe P, Lenoir CJG, MacLeod R, Escudero-Martinez C, Bos JIB (2014) Plant immunity in plant–aphid interactions. *Front Plant Sci* **5**: 663.

Jones L, Seymour GB, Knox JP (1997) Localization of pectic galactan in tomato cell walls using a monoclonal antibody specific to (1 → 4)- β -D-galactan. *Plant Physiol* **113**: 1405-1412

Karkonen A, Kuchitsu K (2015) Reactive oxygen species in cell wall metabolism and development in plants. *Pytochem.***112**: 22–32

Karpinska B, Zhang K, Rasool B, Pastok D, Morris J, Verrall SR, Hedley PE, Hancock RD, Foyer CH (2017) The redox state of the apoplast influences the acclimation of photosynthesis and leaf metabolism to changing irradiance. *Plant Cell Environ* doi: 10.1111/pce.12960

Kasprowicz L, Malloch G, Foster S, Pickup J, Zhan J, Fenton B (2008) Clonal turnover of MACE-carrying peach-potato aphids (*Myzus persicae* (Sulzer), Homoptera: Aphididae) colonizing Scotland. *Bull Ent Res* **98**: 115–124

Kerchev PI, Fenton B, Foyer CH, Hancock RD (2012a) Plant responses to insect herbivory: Interactions between photosynthesis, reactive oxygen species and hormonal signalling pathways. *Plant Cell Environ* **35**: 441-453

Kerchev PI, Fenton B, Foyer CH, Hancock RD (2012b) Infestation of potato (*Solanum tuberosum* L.) by the peach-potato aphid (*Myzus persicae* Sulzer) alters cellular redox status and is influenced by ascorbate. *Plant Cell Environ* **35**: 430-440

Kerchev PI, Karpinska B, Morris JA, Hussain A, Verrall SR, Hedley PE, Fenton B, Foyer CH, Hancock RD (2013) Vitamin C and the abscisic acid-insensitive 4 transcription factor are important determinants of aphid resistance in Arabidopsis. *Antioxidants and Redox Signaling* **18**: 2091-2105

Kimura S, Waszczak C, Hunter K, Wrzaczek M (2017). Bound by fate: the role of reactive oxygen species in receptorlike kinase signaling. *Plant Cell* **29**: 638–654.

Knoblauch M, Froelich DR, Pickard WF, Peters WS (2014) SEORious business: structural proteins in sieve tubes and their involvement in sieve element occlusion. *J Exp Bot* **65**: 1879-1893

Laitinen T, Morreel K, Delhomme N, Gauthier A, Schiffthaler B, Nikolov K, Brader G, Lim K-J, Teeri TH, Street NR, Boerjan W, Kärkönen A (2017) A key role for apoplastic H₂O₂ in Norway spruce phenolic metabolism. *Plant Physiol.* **174**: 1449-1475.

Liang D, Liu M, Hu Q, He M, Qi X, Xu Q, Zhou F, Chen Xm (2015) Identification of differentially expressed genes related to aphid resistance in cucumber (*Cucumis sativus* L.). *Sci. Rep.* **5**: 9645

Leroux O, Sørensen I, Marcus SE, Viane RLL, Willats WGT, Knox JP (2015) Antibody-based screening of cell wall matrix glycans in ferns reveals taxon, tissue and cell-type specific distribution patterns. *BMC Plant Biol* **15**: 56

Lu D, Wang T, Persson S, Mueller-Roeber B, Schippers JHM (2014) Transcriptional control of ROS homeostasis by KUODA1 regulates cell expansion during leaf development. *Nature Comms* **5**: 3767

McCartney L, Steele-King CG, Jordan E, Knox J P (2003) Cell wall pectic (1-4)- β -D-galactan marks the acceleration of cell elongation in the Arabidopsis seedling root meristem. *Plant J* **33**: 447–454

Marcus SE, Blake AW, Benians TAS, Lee KJD, Poyser C, Donaldson L, Leroux O, Rogowski A, Petersen HL, Boraston A, Gilbert HJ, Willats WGT, Knox JP (2010) Restricted access of proteins to mannan polysaccharides in intact plant cell walls. *Plant J* **64**: 191-203

Mai VC, Bednarski W, Borowiak-Sobkowiak, Wilkaniec B, Samardakiewicz S, Morkunas I (2013) Oxidative stress in pea seedling leaves in response to *Acyrtosiphon pisum* infestation. *Phytochem.* **93**: 49–62.

Miller G, Schlauch K, Tam R, Cortes D, Torres MA, Shulaev V, Dangl J, Mittler R (2009) The plant NADPH oxidase RBOHD mediates rapid systemic signaling in response to diverse stimuli. *Science Signal* **2**: ra45

Mittler R (2017) ROS are good. *Trends Plant Sci.* **22**: 11-18.

Mittler R, Vanderauwera S, Suzuki N, Miller G, Tognetti VB, Vandepoele K, Gollery M, Shulaev V, Van Breusegem F (2011) ROS signaling: the new wave? *Trends Plant Sci.* **16**: 300–309.

Moloi M J, van derWesthuizen, A J. (2006) The reactive oxygen species are involved in resistance responses of wheat to the Russian wheat aphid. *J. Plant Physiol.* **163**: 1118–1125.

Mousavi SAR, Chauvin A, Pascaud F, Kellenberger S, Farmer EE (2013) *GLUTAMATE RECEPTOR-LIKE* genes mediate leaf-to-leaf wound signalling. *Nature* **500**: 422-426

Munné-Bosch S, Queval G, Foyer CH (2013) The impact of global change factors on redox signaling underpinning stress tolerance. *Plant Physiol* **161**: 5-19

Müller K, Linkies A, Vreeburg RAM, Fry SC, Krieger-Liszkay A, Leubner-Metzger G (2009) In vivo cell wall loosening by hydroxyl radicals during cress seed germination and elongation growth. *Plant Physiol* **150**: 1855–1865

Nishimura MT, Stein M, Hou BH, Vogel JP, Edwards H, Somerville SC (2003). Loss of a callose synthase results in salicylic acid-dependent disease resistance. *Science* **301**: 969–997.

Noctor G, Foyer CH (2016) Intracellular redox compartmentation and ROS-related communication in regulation and signaling. *Plant Physiol* **171**: 1581–1592

Parsons HT, Fry SC (2012) Oxidation of dehydroascorbic acid and 2,3-diketogulonate under plant apoplastic conditions. *Phytochem* **75**: 41-49

Pastori GM, Kiddle G, Antoniw J, Bernard S, Veljovic-Jovanovic S, Verrier PJ, Noctor G, Foyer CH (2003) Leaf vitamin C contents modulate plant defense transcripts and regulate genes controlling development through hormone signaling. *Plant Cell* **15**: 939–951

Pedersen HL, Fangel JU, McCleary B, Ruzanski C, Rydahl MG, Ralet M-C, Farkas V, von Schantz L, Marcus SE, Andersen MCF, Field R, Ohlin M, Knox JP, Clausen MH, Willats WGT (2012) Versatile high resolution oligosaccharide microarrays for plant glycobiology and cell wall research. *J Biol Chem* **287**: 39429-39438

Pignocchi C, Fletcher JM, Wilkinson JE, Barnes JD, Foyer CH (2003) The function of ascorbate oxidase in tobacco. *Plant Physiol* **132**: 1631-1641

Pignocchi C, Foyer CH (2003) Apoplastic ascorbate metabolism and its role in the regulation of cell signalling. *Curr Opin Plant Biol* **6**: 379-389

Pignocchi C, Kiddle G, Hernández I, Foster SJ, Asensi A, Taybi T, Barnes J, Foyer CH (2006) Ascorbate oxidase-dependent changes in the redox state of the apoplast modulate gene transcript accumulation leading to modified hormone signaling and orchestration of defense processes in tobacco. *Plant Physiol* **141**: 423-435

Prince DC, Drurey C, Zipfel C, Hogenhout SA (2014). The leucine-rich repeat receptor-like kinase BRASSINOSTEROID INSENSITIVE1-ASSOCIATED KINASE1 and the cytochrome P450 PHYTOALEXIN DEFICIENT3 contribute to innate immunity to aphids in *Arabidopsis*. *Plant Physiol* **164**: 2207–2219

Ruiz-May E, Hucko S, Howe KJ, Zhang S, Sherwood RW, Thannhauser TW, Rose JKC (2014) A comparative study of lectin affinity based plant N-glycoproteome profiling using tomato fruit as a model. *Mol Cell Proteomics* **13**: 566-579

Schmiesing A, Emonet A, Gouhier-Darimont C, Reymond P (2016) Arabidopsis MYC transcription factors are the target of hormonal salicylic acid/jasmonic acid cross talk in response to *Pieris brassicae* egg extract. *Plant Physiol* **170**: 2432-2443

Sehrawat A, Deswal R (2014) S-nitrosylation analysis in *Brassica juncea* apoplast highlights the importance of nitric oxide in cold-stress signaling. *J Proteome Res* **13**: 2599-2619

Soylu S, Brown IR, Mansfield JW (2005) Cellular reactions in Arabidopsis following challenge by strains of *Pseudomonas syringae*: from basal resistance to compatibility. *Physiol. Mol. Plant Pathol.* **66**: 232–243.

Suzuki N, Miller G, Morales J, Shulaev V, Torres MA, Mittler R (2011) Respiratory burst oxidases: the engines of ROS signalling. *Current Opin. Plant Biol.* **14**: 691–699.

Sytykiewicz H (2016) Deciphering the role of NADPH oxidase in complex interactions between maize (*Zea mays* L.) genotypes and cereal aphids. *Biochem Biophys Res Commun.* **476**: 90-95

Tang D, Wang G, Zhou J-M (2017). Receptor kinases in plant-pathogen interactions: more than pattern recognition. *Plant Cell* **29**: 618–637

Tenhaken R (2015) Cell wall remodeling under abiotic stress. *Front Plant Sci* **5**: 771

Tjallingii WF (2006) Salivary secretions by aphids interacting with proteins of phloem wound responses. *J Exp Bot* **57**: 739-745

- Ueda Y, Siddique S, Frei M** (2015) A novel gene, OZONE-RESPONSIVE APOPLASTIC PROTEIN1, enhances cell death in ozone stress in rice. *Plant Physiol* **169**: 873–889
- Verhertbruggen Y, Marcus SE, Haeger A, Ordaz-Ortiz JJ, Knox JP** (2009) An extended set of monoclonal antibodies to pectic homogalacturonan. *Carbohydr Res* **344**: 1858-1862
- War AR, Paulraj MG, Ahmad T, Buhroo AA, Hussain B, Ignacimuthu S, Sharma HC** (2012) Mechanisms of plant defense against insect herbivores. *Plant Signal Beh* **7**: 1306-1320
- Will T, van Bel, AJE** (2006) Physical and chemical interactions between aphids and Plants. *J Exp Bot* **57**: 729–737
- Will T, Kornemann SR, Furch ACU, Tjallingii WF, van Bel AJE** (2009) Aphid watery saliva counteracts sieve-tube occlusion: a universal phenomenon? *J Exp Biol* **212**:3305-3312
- Zielinska DF, Gnad F, Schropp K, Wiśniewski JR, Mann M** (2012) Mapping N-glycosylation sites across seven evolutionarily distant species reveals a divergent substrate proteome despite a common core machinery. *Mol Cell* **46**: 542-548

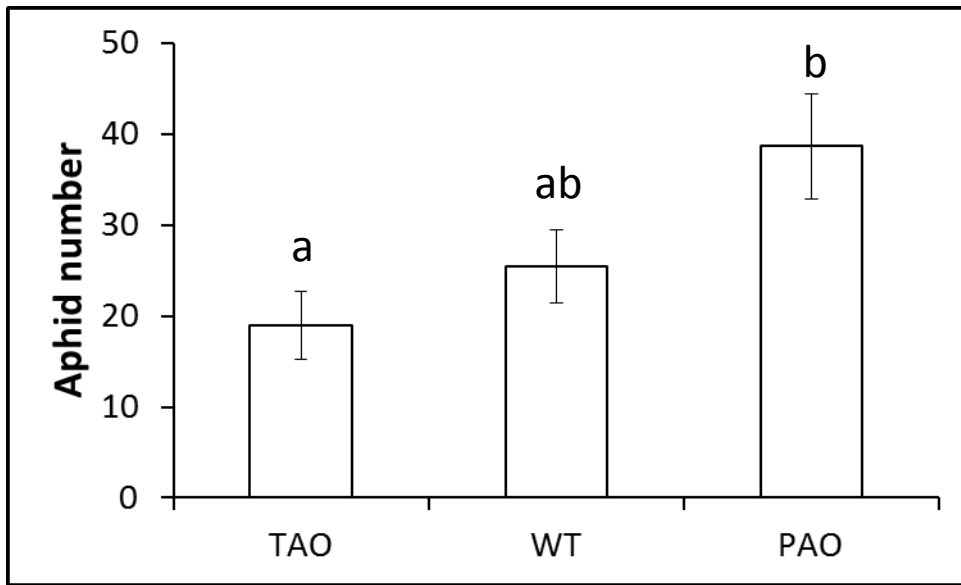


Figure 1 Impact of manipulation of ascorbate oxidase transcripts on aphid fecundity in tobacco. Six week old WT, PAO and TAO plants were infested with single 1 day old nymph of *Myzus persicae* and cultured for 14 days as described. The total number of aphids present after 14 days infestation is indicated as mean \pm SE (n =6). Different letters indicate significant differences between values as determined by one-way ANOVA with Fishers protected LSD test ($P < 0.05$).

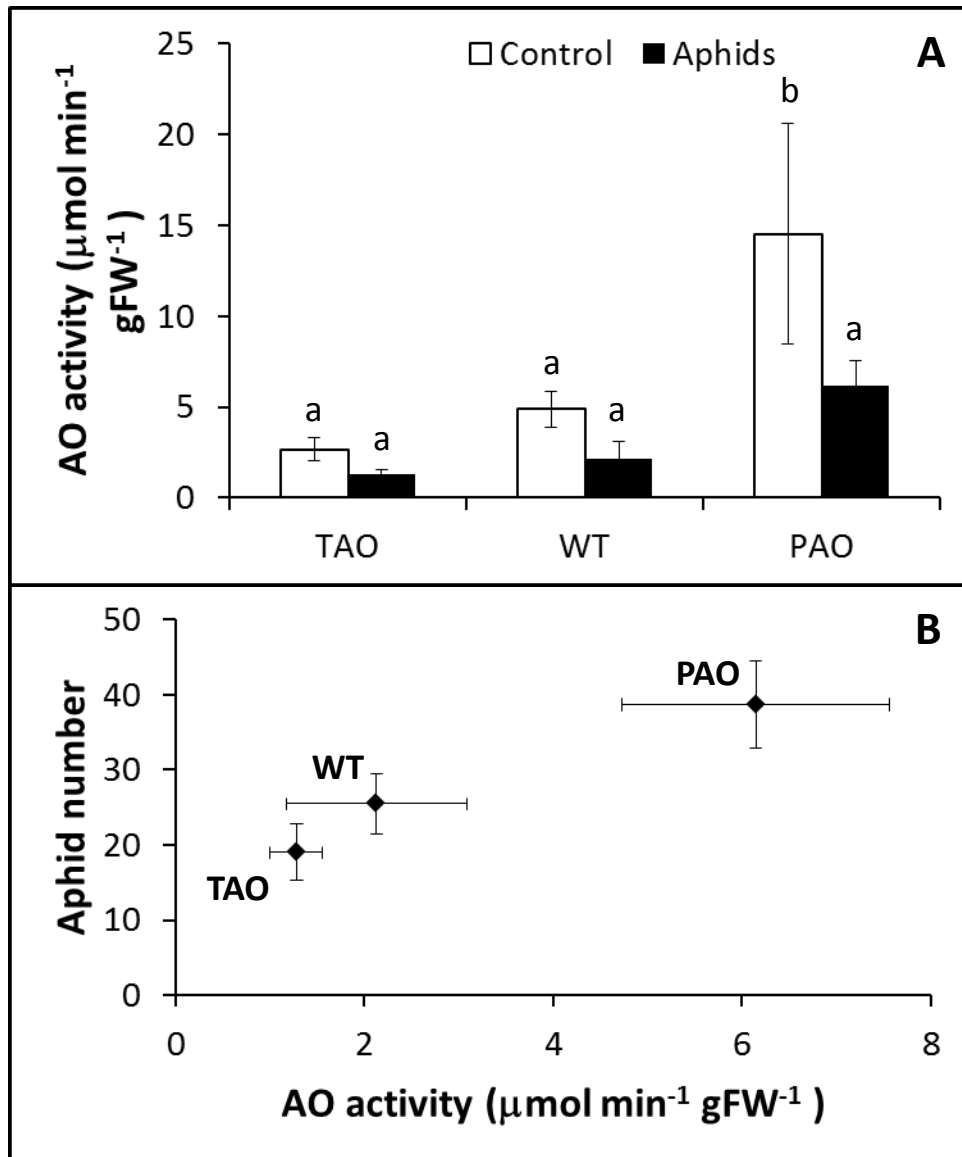


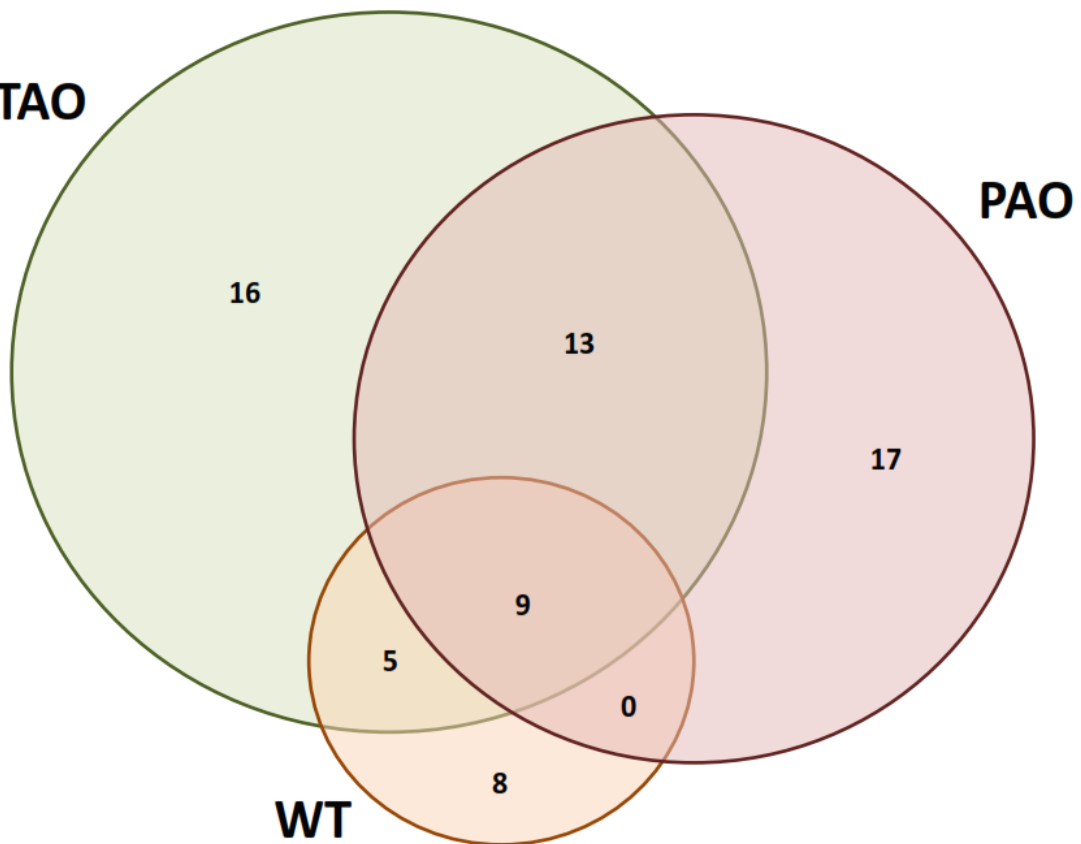
Figure 2 Impact of aphid infestation on apoplastic ascorbate oxidase activity in tobacco leaves. WT, PAO and TAO tobacco plants were grown for six weeks in the absence of aphids. At the end of the six week period, one group of plants were infested with a single one-day old nymph while the remaining group were left in the absence of aphids and grown in cages for further two week as described. At the end of the two week period plants were harvested and apoplastic ascorbate oxidase activity quantified as described (A). Bars illustrate mean AO activity \pm SE (n = 6) and different letters above bars indicate values that were significantly different from one another according to Fishers protected LSD test. A linear relationship was observed between measured ascorbate oxidase activity and aphid fecundity (B).

TAO

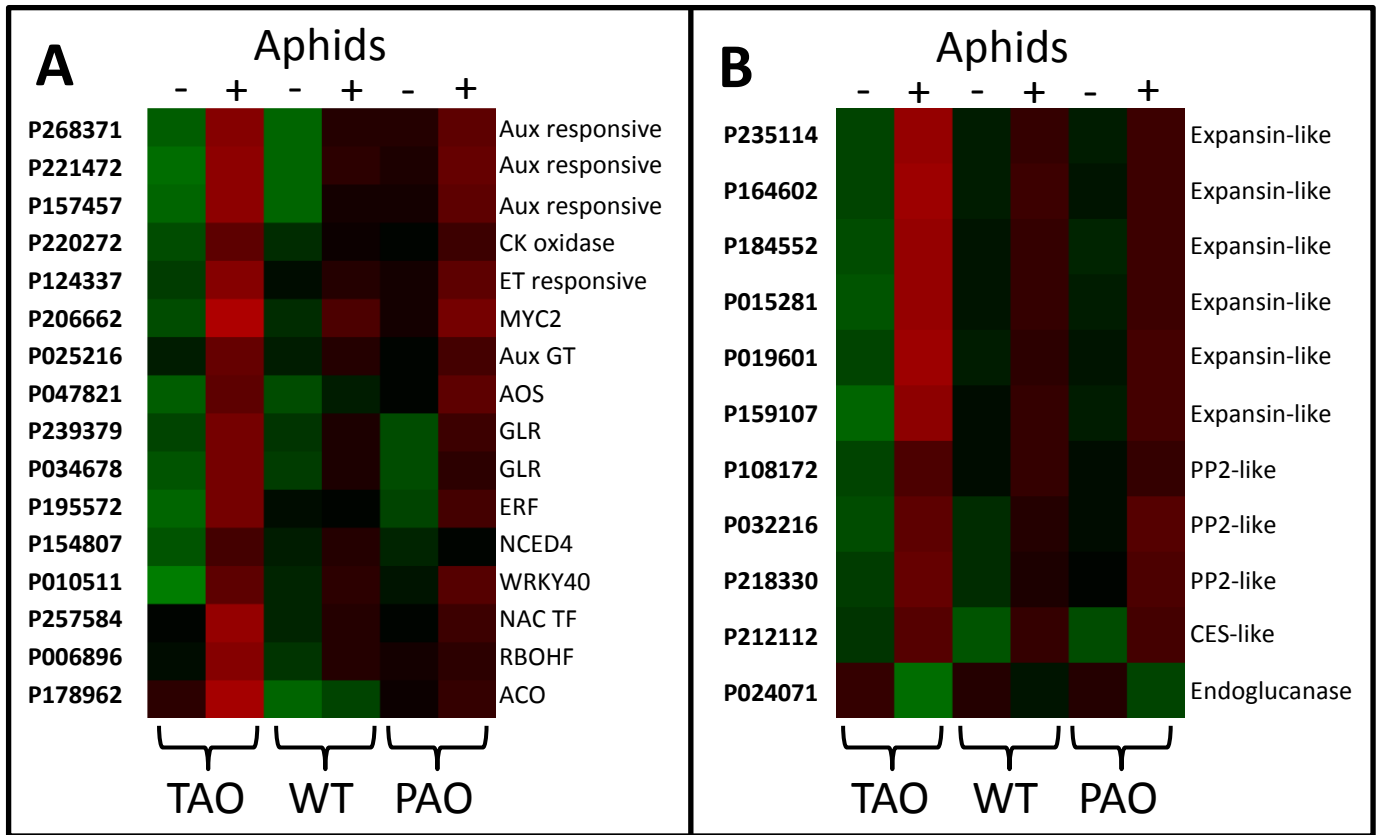


A

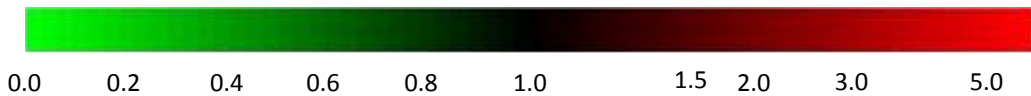
TAO



B



Relative abundance



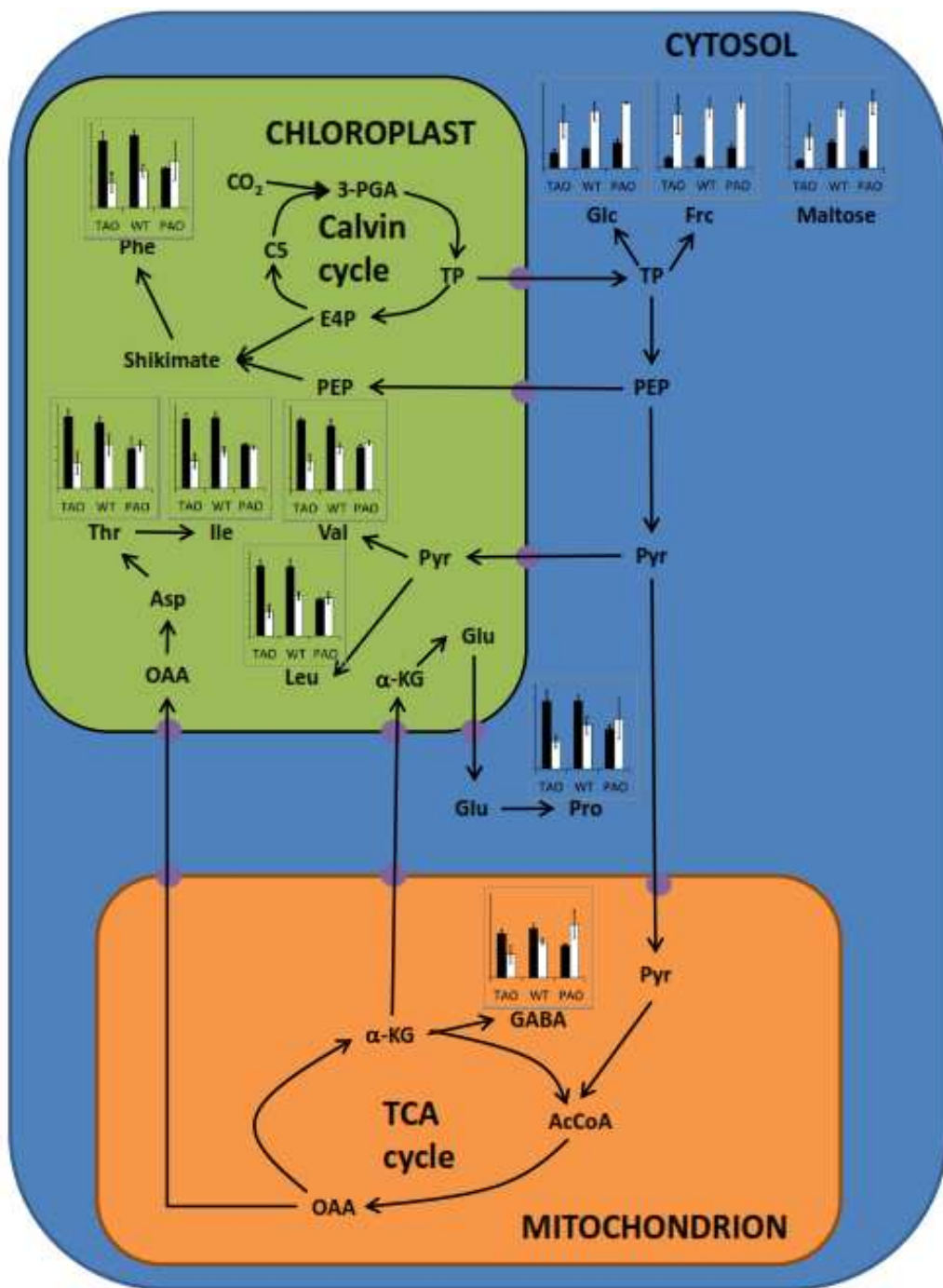


Figure 5 Influence of aphid infestation on leaf content of amino acids and sugars

Bar charts indicate the relative concentrations of amino acids and sugars significantly altered in abundance in leaves in response to aphid infestation and refer to antisense TAO, wild-type (WT) and sense PAO plants as indicate. Black bars indicate concentration in the absence of aphids and white bars in the presence of aphids and data are represented as mean \pm SE, n = 3. The figure indicates compartmentation and metabolic relationships between different compounds and presumed transporters are indicated as purple circles. 3-PGA, 3-phosphoglycerate; TP, triose phosphates; E4P, erythrose-4-phosphate; C5, five carbon Calvin pathway intermediates; PEP, phosphoenolpyruvate; Pyr, pyruvate; AcCoA, acetyl-coenzyme A; OAA, oxaloacetate; α -KG, α -ketoglutarate; GABA, γ -amino butyrate; Glc, glucose; Frc, fructose. Amino acids are indicated according to their standard 3 letter abbreviation.

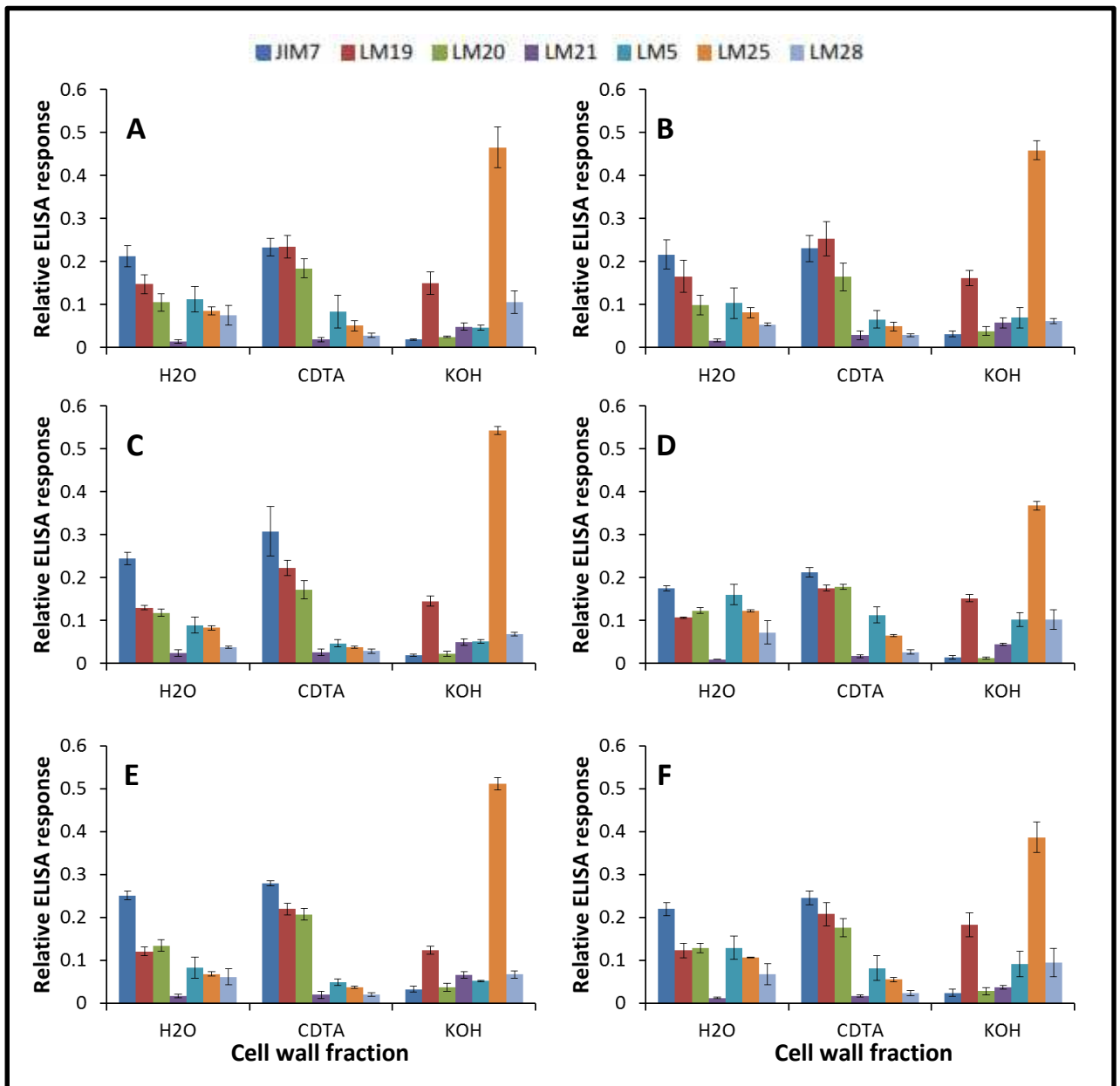


Figure 6 Influence of aphid infestation on cell wall epitopes in tobacco leaves

TAO (A,B), wild-type (C,D) and PAO (E,F) plants were either grown in the absence (A, C, E) or presence (B, D, F) of aphids for 15 days prior to the preparation of cell walls as alcohol insoluble residues. Water (H2O), CDTA and KOH extracts were prepared as described and the relative abundance of wall epitopes was estimated following probing with specific antibodies as shown. Graphs represent the relative ELISA response for each antibody estimated as the absorbance measured following incubation with HRP substrate divided by the sum of absorbances following probing with each of the antibodies. Data are presented as mean \pm SE, $n = 3$.